Karlsruhe Institute of Technology

Institute of Mechanics

Talcum Particle Modified Thermoplastics
Part II: Computational Modeling

Philipp Hempel, Thomas Seelig

13. Problemseminar

,,Deformation und Bruchverhalten von Kunststoffen”

Merseburg, Juni 2011

Institute of Mechanics
Kaiserstr. 12
D-76131 Karlsruhe
Tel.: +49 (0) 721/ 608-42071
Fax: +49 (0) 721/608-47990
E-Mail: info@ifm.kit.edu
www.ifm.uni-karlsruhe.de

Talcum Particle Modified Thermoplastics Part II: Computational Modeling

P. Hempel, Th. Seelig
Institute of Mechanics, Karlsruhe Institute of Technology, Karlsruhe

Summary: A constitutive model for talc-particle modified thermoplastic polymers is presented. Motivated by experimental observations, the model accounts for anisotropy, pressure, temperature and strain rate dependence, as well as damage induced plastic dilatancy under tensile loading. After implementation into a commercial finite element code, the model is validated by simulation of 3-point-bending tests on injection moulded plates.

Introduction – experimental findings

Thermoplastic polymers modified with mineral (e.g. talc) particles are widely used in technical applications. Correspondingly, their mechanical behavior has been investigated in a number of experimental studies, e.g. (Diez-Gutierrez et al., 1999a,b; Guerrica-Echevarria et al., 1998; Hadal & Misra, 2004; Jerabek et al., 2010; Stamhuis, 1984; Vollenberg & Heikens, 1990; Zihlif & Ragosta, 1991). However, an adequate material model that allows for the reliable structural analysis of technical components in the framework of finite element simulations so far seems to be lacking. In the present paper, a respective constitutive model is presented and discussed. Its calibration is based on the recent experimental study of a talcum-modified polypropylene (PP) discussed in detail in (Kunkel & Becker, 2011); the key findings of this work are briefly summarized below.

The deformation behavior of the material under uniaxial quasistatic tension at room temperature is shown in Fig. 1a in terms of true stress vs. logarithmic strain curves and the variation of Poisson's ratio in the course of deformation. The curves refer to two perpendicular directions of the material, i.e. the principal flow ("longitudinal") direction of the preceding manufacturing (injection moulding) process and the "transverse" direction. From both, the stress and Poisson's ratio, a pronounced anisotropy of the material behaviour can be seen; for instancs, the yield stress is higher in the longitudinal direction. This anisotropy may be ascribed to the anisotropic microstructure typically observed in talc-particle modified thermoplastics with the platelet-like particles oriented with the flow direction (Heise et al., 1982; Stamhuis, 1984; Hadal & Misra, 2004; Kunkel & Becker, 2011), see also Fig. 1b. Poisson's ratio (taken here as the ratio of total strains) in both directions decreases from the initial (elastic) value of about 0.3 to significantly

lower values in the course of deformation. This indicates an overall dilatant behavior in the plastic range whereas the PP matrix is known to be plastically incompressible. The reason for this overall volume increase under tensile loading lies in massive particle-matrix debonding and subsequent void growth as seen, for instance, in micrographs in (Hadal & Misra, 2004). This damage mechanism may also be responsible for the slight softening upon the onset of yield (Fig. 1a) which is not displayed by neat PP. Moreover, the progressive hardening of neat PP appears to be leveled off by the damage in PP-talc so that a plateau-like stress response in the large strain regime results (Fig. 1a). Finally, owing to the thermoplastic matrix a pronounced temperature and strain rate dependence of PP-talc is observed (Kunkel & Becker, 2011).

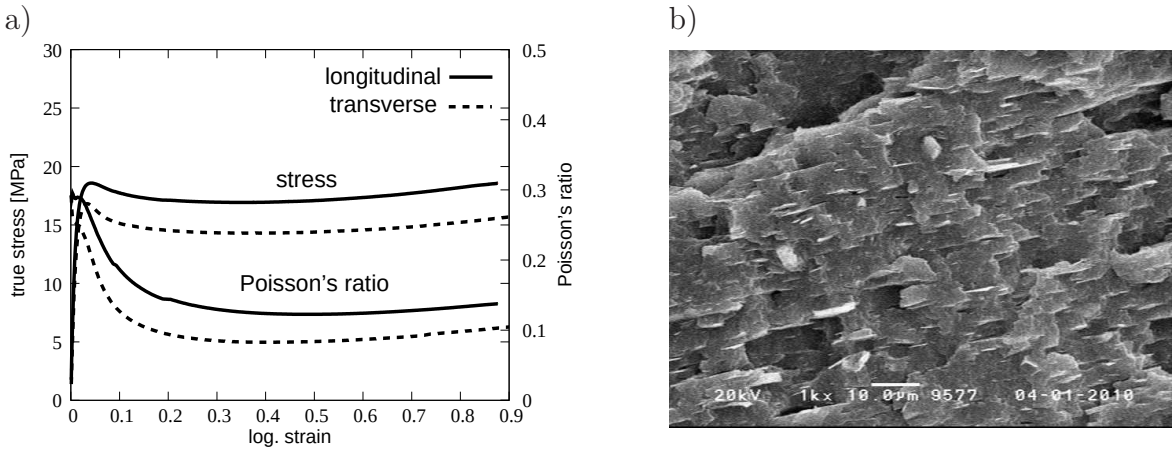

Figure 1: a) Deformation behaviour in terms of stress-strain response and Poisson's ratio (indicating plastic dilatancy), b) microstructure of talc-modified PP (Kunkel & Becker, 2011)

With a special focus on polymers, an anisotropic pressure dependent yield criterion has been suggested in (Cadell et al., 1973). Such a yield criterion alone, however, does not capture the complex softening-rehardening behavior including damage and plastic dilatancy in the post-yield regime of the material considered in the present work.

Constitutive modeling

The material model developed here aims at describing the deformation behavior of PP-talc at large strains. The small strain behavior therefore is for simplicity taken isotropic and purely elastic. It is written in rate form as

$$\overset{\nabla}{\boldsymbol{\sigma}} = \mathbf{E} : (\boldsymbol{D} - \boldsymbol{D}^p) \tag{1}$$

where $\overset{\nabla}{\boldsymbol{\sigma}}$ denotes the Jaumann rate of the Cauchy stress tensor, $\boldsymbol{D}$ is the strain rate tensor, $\boldsymbol{D}^p$ its plastic part, and $\mathbf{E}$ is the isotropic forth order elasticity tensor which involves the

temperature dependent Young's modulus $E(T)$ and the elastic Poisson's ratio ν. The plastic strain rate tensor is computed from the flow rule

$$\boldsymbol{D}^p = \dot{\varepsilon}_p \frac{\partial \Psi}{\partial \boldsymbol{\sigma}} \tag{2}$$

with the equivalent plastic strain rate

$$\dot{\varepsilon}_p = \dot{\varepsilon}_0 \langle \Phi \rangle^{1/r} \tag{3}$$

determined by the yield function

$$\Phi(\boldsymbol{\sigma}) = \underbrace{\sqrt{\boldsymbol{\sigma} : \mathbf{A} : \boldsymbol{\sigma}}}_{\Psi} - g(T)(1-f) \; - \; c \, \langle -\mathrm{tr}\boldsymbol{\sigma} \rangle \tag{4}$$

in conjunction with a reference strain rate $\dot{\varepsilon}_0$ and a rate sensitivity parameter r. Since only part of the yield function serves as the flow potential $\Psi(\boldsymbol{\sigma})$ in the flow rule, the (visco-) plasticity model set up here is non-associated. The so-called Macauley brackets $\langle ... \rangle$ used above have the property

$$\langle x \rangle = \left\{ \begin{array}{lcl} x & , & x \geq 0 \\ 0 & , & x < 0 \end{array} \right\} \quad . \tag{5}$$

The parameter c in (4) accounts for the pressure dependence of the yield strength; it is only "active" for compressive loading ($\mathrm{tr}\boldsymbol{\sigma} < 0$). The function $g(T)$ in (4) captures the temperature dependence of the yield strength, and the damage variable f represents the porosity which evolves according to

$$\dot{f} = (1-f)\mathrm{tr}\boldsymbol{D}^p \quad . \tag{6}$$

The forth order tensor $\mathbf{A}$ in (4) accounts for the anisotropic yield behavior. In the simplest case of transverse isotropy assumed here with only one distinguished material direction (the "longitudinal" direction) it contains five independent parameters.

Model calibration

In a cartesian coordinate system with the 1-axis aligned with the material's "longitudinal" direction the yield function (4) can be written as

$$\begin{aligned} \Phi \;\; = \;\; & \Big[a_{11}\sigma_{11}^2 + a_{22}(\sigma_{22}^2 + \sigma_{33}^2 + 2\sigma_{23}^2) + 2a_{12}\,\sigma_{11}(\sigma_{22} + \sigma_{33}) + \\ & 2a_{23}(\sigma_{22}\sigma_{33} - \sigma_{23}^2) + a_{44}(\sigma_{12}^2 + \sigma_{13}^2) \Big]^{1/2} - \; g(T)(1-f) \; - \; c \, \langle -\mathrm{tr}\boldsymbol{\sigma} \rangle \quad . \end{aligned} \tag{7}$$

From this representation it can be seen that the parameters a_{11} and a_{22} are directly related to the yield strengths under uniaxial tension in the 1-direction and the 2(3)-direction,

respectively, since $\sigma_{11} > 0$ or $\sigma_{22} > 0$ then are the only non-zero stress components. Starting from initial values a_{11_0} and a_{22_0} at the onset of yield, the parameters a_{11} and a_{22} are taken to evolve with the accumulated plastic strain ε^p to capture the experimentally observed post-yield hardening behavior at different testing temperatures according to

$$a_{11} = \frac{a_{11_0}}{1 + h_1(T)\varepsilon_p^{n_1}} \qquad , \qquad a_{22} = \frac{a_{22_0}}{1 + h_2(T)\varepsilon_p^{n_2}} \tag{8}$$

with exponents n_1 and n_2. The parameter a_{12} is adjusted to fit Poisson's ratio in the post-yield regime by evaluating the flow rule (2) for uniaxial tension. Determination of the remaining two parameters a_{23} and a_{44} would require so-called off-axis tests (i.e. tension in a direction not aligned with a principal material direction) or shear tests. Since currently respective data are not available, the assumptions

$$a_{23} = a_{12} \qquad \text{and} \qquad a_{44} = 2(a_{22} - a_{12}) \tag{9}$$

are made which correspond to a von Mises-like behavior. Tensile tests in (Kunkel & Becker, 2011) used here have been performed at three different temperatures, i.e. $-35°$C, room temperature (RT), and 80°C, and the functions $g(T)$, $h_1(t)$, $h_2(T)$ are represented by a bi-linear fit between respective values at the testing temperatures.

The response of the material model in comparison with experimental data is shown in Figs. 2 and 3 for uniaxial tension tests at the three different testing temperatures and in Fig. 4 for uniaxial compression at room temperature. The model well captures the anisotropic and temperature dependent behavior in terms of the true stress-strain curves as well as Poisson's ratio in the large deformation regime. Remarkably, the amount of

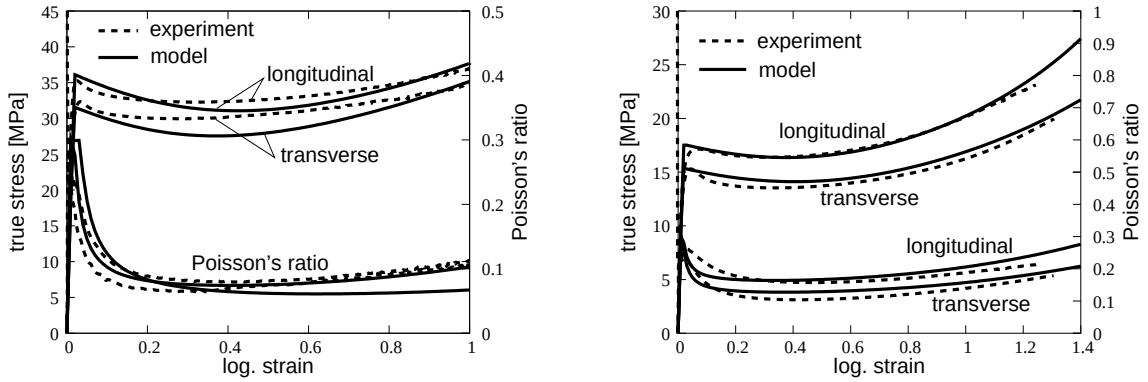

Figure 2: Uniaxial tension at a) $-35°$ C, b) room temperature; experimental data from (Kunkel & Becker, 2011)

plastic dilatancy (seen from Poisson's ratio) strongly depends on temperature. At higher temperatures it is significantly reduced which indicates a smaller amount of particle-matrix debonding and subsequent void growth.

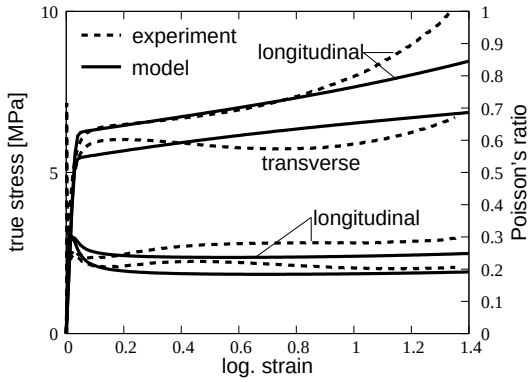

Figure 3: Uniaxial tension at 80° C; experimental data from (Kunkel & Becker, 2011)

The parameter c in the yield function (4) is adjusted to fit the yield strength of the material in uniaxial compression tests at room temperature (Fig. 4). Furthermore, corresponding to the experimental findings from these tests, the material model is taken to display isotropy and plastic incompressibility in the compressive regime.

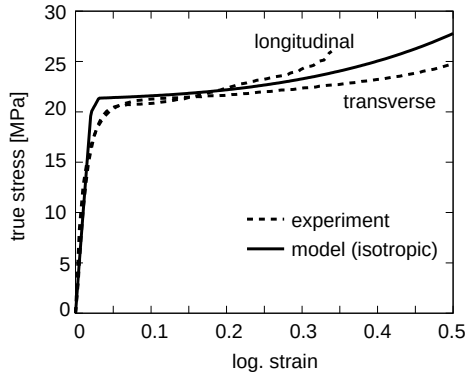

Figure 4: Uniaxial compression at RT; experimental data from (Kunkel & Becker, 2011)

Slight deviations between experimental data and the model response in Figs. 2 to 4 have to be seen in the light of the large temperature range covered and the limited number of material parameters involved. Determination of the latter was accomplished in a relatively easy manner "by hand" and did not require an advanced optimization procedure. The material model has been implemented as a user subroutine in the commercial finite element code LS-Dyna for solid and shell elements.

Validation – simulation of 3-point-bending tests

For validation purposes, 3-point-bending tests at room temperature have been performed on bar-shaped specimens of the above PP-talc material; see (Kunkel & Becker, 2011) for

details. These specimens were taken from injection moulded plates in two perpendicular directions, i.e. the “longitudinal” and the ”transverse” direction. The bending tests were simulated using the material model described above with material parameters calibrated solely from the uniaxial tension and compression tests. The finite element model of the experimantal set-up is shown in Fig. 5

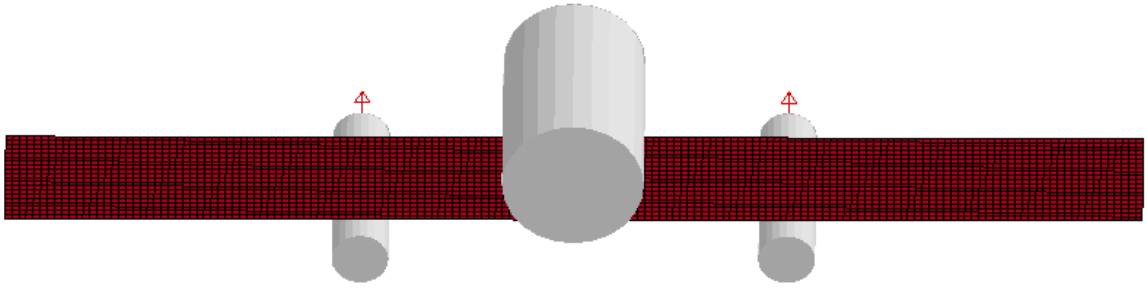

Figure 5: Finite element model of 3-point-bending test

Experimental and numerical results are shown together in Fig. 6a and b for the two material directions. The anisotropy of the material is present also in the bending behaviour, and the computational model well captures this effect.

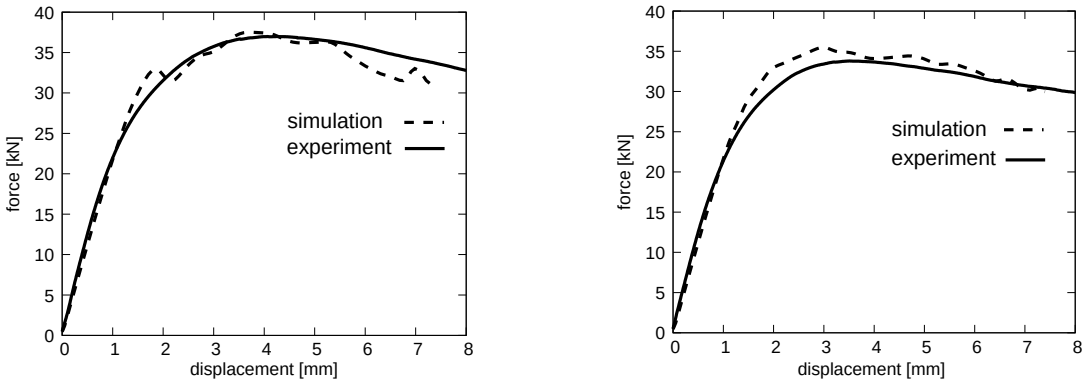

Figure 6: Load-displacement curves of 3-point-bending tests: a) longitudinal direction, b) transverse direction; experimental data from (Kunkel & Becker, 2011)

Discussion and conclusions

Based on experimental data for a talc-particle modified polypropylene, a material model has been developed that accounts for the complex mechanical behavior of thermoplastic polymers containing stiff mineral particles. Special emphasis was laid on the processing-induced anisotropy and the plastic dilatancy under tensile loading. While the latter can

clearly be ascribed to particle-matrix debonding and void growth, the microstructural origin of the macroscopic anisotropy is not fully understood. The overall anisotropy of the material may be due to the anisotropic microstructure with platelet-like particles oriented with the flow direction during injection moulding. It may, however, also result from the crystallinity of the matrix material (PP) which is likewise known to be affected by the preceding flow process (e.g. Fujiyama et al., 1977; Choi & Kim, 2004).

Acknowledgment

Financial support of this work by the ,,Arbeitsgemeinschaft industrieller Forschung" (AiF) under grant no. 15826 N is gratefully acknowledged.

References

Cadell, M.C., Raghava, R.S., Atkins, A.G., 1973. A yield criterion for anisotropic and pressure dependent solids such as oriented polymers. J. Mat. Sci. 8, 1641-1646.

Choi, W., Kim, S.C., 2004. Effects of talc orientation and non-isothermal crystallization rate on crystal orientation of polypropylene in injection-molded polypropylene/ethylene-propylene rubber/talc blends. Polymer 45, 2393-2401.

Diez-Gutierrez, S., Rodriguez-Perez, M.A., De Saja, J.A., Velasco, J.I., 1999a. Dynamic mechanical analysis of injection-moulded discs of polypropylene and untreated and silane-treated talc-filled polypropylene composites. Polymer 40, 5345-5353.

Diez-Gutierrez, S., Rodriguez-Perez, M.A., De Saja, J.A., Velasco, J.I., 1999b. Heterogeneity and anisotropy of injection-molded discs of polypropylene and polypropylene composites. J. Appl. Pol. Sci. 77, 1275-1283.

Fujiyama, M., Awaya, H., Kimura, S., 1977. Mechanical anisotropy in injection-moulded polyproylene. J. Appl. Pol. Sci. 21, 3291-3309.

Guerrica-Echevarria, G., Eguiazabal, J.I., Nazabal, J., 1998. Influence of molding conditions and talc content on the properties of polypropylene composites. Eur. Polym. J. 34, 1213-1219.

Hadal, R.S., Misra, R.D.K., 2004. The influence of loading rate and concurrent microstructural evolution in micrometric talc- and wollastonite-reinforced high isotactic polypropylene composites. Mat. Sci. Engng. A 374, 374-389.

Heise, B., Klostermann, L., Woebcken, W., 1982. Technologische Eigenschaften von Polypropylen-Formteilen im Zusammenhang mit Orientierungen von Zusatzstoffen und

Kristallen. Colloid & Polymer Sci. 260, 487-501.

Jerabek, M., Major, Z., Renner, K., Moczo, J., Pukanszky, B., Lang, R.W., 2010. Filler/matrix-debonding and micro-mechanisms of deformation in particulate filled polypropylene composites under tension. Polymer 51, 2040-2048.

Kunkel, F., Becker, F., 2011. Talcum Particle Modified Thermoplastics. Part I: Experimental Characterization. 13. Problemseminar ,,Deformation und Bruchverhalten von Kunststoffen", Merseburg.

Stamhuis, J.E., 1984. Mechanical properties and morphology of polypropylene composites. Talc-filled, elastomer-modified polypropylene. Polymer Composites 5, 202-207.

Vollenberg, P.H.Th., Heikens, D., 1990. The mechanical properties of chalk-filled polypropylene: a preliminary investigation. J. Mat. Sci. 25, 3089-3095.

Zihlif, A.M., Ragosta, G., 1991, Mechanical properties of talc-polypropylene composites. Materials Letters 11, 368-372.